

# Uniplanar deformation of isotactic polypropylene: 2. Phase structure

Satoshi Osawa\* and Roger S. Porter†

Polymer Science and Engineering Department, University of Massachusetts, Amherst, MA 01003, USA

(Received 9 November 1992; revised 24 February 1993)

The phase structures of uniplanar-drawn isotactic polypropylene (iPP) have been investigated. Three phases ( $\alpha$ -crystal, smectic and amorphous) are found to coexist in the uniaxially compressed samples. From thermal analyses and density measurements, the fractions and densities of these phases have been evaluated. At a compression draw temperature of  $50^\circ\text{C} < T_d$  (the upper smectic phase stability limit), the amount of  $\alpha$ -crystal decreased significantly and the smectic phase increased on developing a compression ratio up to  $\sim 10$ . The transition energy for smectic to crystal phase was found to be  $\sim 5.5 \text{ cal g}^{-1}$ . At a draw temperature  $> T_d$ , decrystallization without smectic phase stability proceeded during the deformation. No draw-induced crystallization was observed. At all deformation temperatures, the density of the amorphous phase increased in the initial stage of deformation reaching a limit on further draw.

(Keywords: planar deformation; smectic phase; isotactic polypropylene)

## INTRODUCTION

Uniaxial drawing of flexible chain polymers has been extensively studied to enhance their mechanical and physical properties<sup>1,2</sup>. Among thermoplastics, isotactic polypropylene (iPP) has been drawn uniaxially to high levels<sup>3-5</sup>. The consequent properties in the transverse direction, however, are less than those of the unoriented polymer. Biaxial deformation, on the other hand, can lead to enhancement of properties in two directions. A simple uniplanar compression can create a perfect equibiaxial field in the plane perpendicular to the compression axis<sup>6</sup>.

In this study, iPP has been uniaxially compressed by a forging (uniplanar) process. The resultant sample consisted of two or three phases ( $\alpha$ -crystal and amorphous, or  $\alpha$ -crystal, amorphous and smectic), depending on the draw temperature. The phase structures have been characterized by thermal analyses and density measurements. The amount of the smectic phase was found to increase as deformation proceeded at a draw temperature of  $50^\circ\text{C} < T_d$  (the smectic phase stability temperature). The amorphous density increased with increasing compression draw ratio. Based on these results, the deformation mechanism for the compressive uniplanar draw of iPP is discussed.

## EXPERIMENTAL

Moulded iPP sheet was uniaxially compressed under a constant compression speed of  $0.254 \text{ cm min}^{-1}$  using an INSTRON model 1333. A detailed description of iPP and the compression test have been given<sup>7,8</sup>. Thermal

analyses were performed on a Perkin-Elmer DSC7 calorimeter. All scans were recorded at a heating rate of  $20^\circ\text{C min}^{-1}$ . Density measurements were made on a density gradient column, using ethyl alcohol and a sodium bromide aqueous solution as a mixed miscible solvent pair. Wide-angle X-ray scattering (WAXS) patterns were obtained with a Statton camera using Ni-filtered  $\text{Cu K}\alpha$  radiation.

## RESULTS AND DISCUSSION

On uniaxial compression of iPP, the smectic phase is induced at draw temperatures ( $T_d$ ) below the upper temperature limit for smectic phase stability ( $T_s$ ). The  $T_s$  for deformation under this experimental condition is  $\sim 120^\circ\text{C}$ <sup>7</sup>. Therefore, the compression drawn samples prepared at  $T_d < T_s$  consist of  $\alpha$ -crystal, amorphous and smectic regions. No smectic phase is observed in samples prepared at  $T_d > 70^\circ\text{C}$ , since the smectic phase induced under deformation reverts back to  $\alpha$ -crystals<sup>7,9</sup>. In this study, a  $T_d$  of 50, 100 and  $140^\circ\text{C}$  was taken. To characterize the fraction and density of the phases, a two-phase model can be applied for the  $T_d$  of 100 and  $140^\circ\text{C}$  using equation (1). For the  $T_d$  of  $50^\circ\text{C}$ , at least a three-phase model is required; thus, equation (2) may be used for estimations:

$$\frac{1}{\rho} = \frac{X_c}{\rho_c} + \frac{1 - X_c}{\rho_a} \quad (1)$$

$$\frac{1}{\rho} = \frac{X_c}{\rho_c} + \frac{X_s}{\rho_s} + \frac{1 - (X_c + X_s)}{\rho_a} \quad (2)$$

where  $\rho$  is the density of the sample, and the subscripts c, s and a represent the crystal, smectic and amorphous phases, respectively.  $X_c$ ,  $X_s$  and  $1 - (X_c + X_s)$  are weight fractions of the crystal, smectic and amorphous phases, respectively.

\* Present address: Department of Materials Science and Technology, Science University of Tokyo, Yamaguchi College, Daigakudori, Onodashi, Yamaguchi 756, Japan

† To whom correspondence should be addressed

Figure 1 shows the heat of fusion ( $\Delta H$ ) of drawn samples as a function of compression draw ratio (CR) for the samples prepared at a  $T_d$  of 100 and 140°C. The crystallinity ( $\alpha$ -crystal content) decreases as the deformation proceeds. For  $T_d=140^\circ\text{C}$ , the  $\Delta H$  of the drawn sample is higher than that of original sample; that is, the samples are annealed at 140°C. However,  $\Delta H$  decreased with draw. This suggests that decrystallization also proceeds during deformation. This is in contrast to uniaxially drawn iPP with no significant change in crystallinity<sup>10</sup> or with an increase in crystallinity<sup>11,12</sup>. Figure 2 shows  $\rho$  as a function of CR; for all  $T_d$ , the value of  $\rho$  decreased with CR. As shown in Figure 3, the crystal modification of deformed and subsequently heat-treated samples was found by WAXS to be of the  $\alpha$ -form and the lattice constant did not change significantly, indicating no change in the  $\alpha$ -crystal density during the deformation.

There seem to be two effects on  $\rho$  in the experimental range studied. The first is decrystallization during the early stage of deformation (see Figure 1), and the second is an increase in amorphous density due to the compression deformation. For samples prepared at a  $T_d$  of 100 and 140°C, and for the subsequently heat-treated

(140°C for 30 min) samples at a  $T_d$  of 50, 100 and 140°C, the amorphous densities ( $\rho_a$ ) can be estimated using equation (1), since these samples must consist of only  $\alpha$ -crystal and amorphous phases. After the heat treatment,  $\Delta H$  of the samples at a  $T_d$  of 100 and 140°C increased by  $\sim 3$  and  $\sim 1$  cal  $\text{g}^{-1}$ , respectively.  $X_c$  ( $\alpha$ -crystal content) was evaluated from  $\Delta H/\Delta H_c^\circ$ , where  $\Delta H_c^\circ$  is the heat of fusion of a perfect iPP crystal. In the calculation, it is necessary to select  $\Delta H_c^\circ$  and the density for the perfect  $\alpha$ -crystal.

Several values of  $\Delta H_c^\circ$  have been reported. Roy *et al.*<sup>13</sup> reported that the percentages of crystallinity based on heat of fusion ( $\Delta H_c^\circ=33$  cal  $\text{g}^{-1}$ ) and on density measurements were very consistent; that is, the relation between  $1/\rho$  (specific volume) and  $X_c$  is linear if the amorphous density and crystal density are constant. Figure 4 shows  $1/\rho$  versus  $X_c$  for data from Figures 1 and 2. In Figure 4,  $X_c$  was calculated from two reported  $\Delta H_c^\circ$  values of 33 and 50 cal  $\text{g}^{-1}$ <sup>14,15</sup>. The extrapolated crystal densities from undeformed samples are 0.938 and 0.996  $\text{g cm}^{-3}$  for 33 and 50 cal  $\text{g}^{-1}$ , respectively. The reported values<sup>15</sup> for  $\alpha$ -crystal density are  $\sim 0.932$ – $0.946$   $\text{g cm}^{-3}$ . In the calculation using equation (1), values of  $\Delta H_c^\circ=33$  cal  $\text{g}^{-1}$  and  $\rho_c=0.938$   $\text{g cm}^{-3}$  were taken for the perfect crystal. The results for calculation of  $\rho_a$  are shown in Figure 5. It can be seen that the value of  $\rho_a$  increases with CR up to  $\sim 10$ , independent of  $T_d$ . This result, combined with information in Figure 1, indicates that the compression of the amorphous region and decrystallization proceed simultaneously during the initial stage of deformation ( $CR < 10$ ). For  $T_d=100^\circ\text{C}$ , the  $\rho_a$  seems to be relatively low and goes down at high CR ( $> 20$ ). At 100°C, the smectic phase is induced during the deformation, but then reverts back to the  $\alpha$ -crystal. However, the sample may have a small amount of smectic phase (but unmeasurable by d.s.c.) especially for a high CR. The existence of the smectic phase lowers  $\rho$  since the density of the smectic phase is lower than that of the  $\alpha$ -crystal. In this case,  $\rho_a$  is calculated as a lower value using equation (1). When samples are subsequently annealed at 140°C, the residual smectic phase should revert back to the  $\alpha$ -crystal. In fact, the estimated  $\rho_a$  of the annealed sample is higher than that of the unannealed one for  $T_d=100^\circ\text{C}$ . The data in Figure 5 are scattered. This may be due to the lower accuracy of the density measurement and/or the d.s.c. measurement. In our prior study<sup>16</sup>, the sample densities were estimated using a density gradient column with an organic solvent pair (carbon tetrachloride and hexane), which reduced data scatter. However, some solvent was taken up by the samples. Therefore, the  $\rho_a$  values in the prior study were a few per cent higher than those in Figure 5. It should be noted that this increase in amorphous density with compressive draw is a new finding.

Figure 6 shows the d.s.c. thermogram for the sample at  $T_d=50^\circ\text{C}$  and  $CR=10$ . The exotherm for formation of the smectic phase ( $\Delta H_s$ ) was observed at around 80°C. The smectic phase reverts back to the  $\alpha$ -crystal after the exotherm (since the exothermic process is a transition from smectic to  $\alpha$ -crystal), followed by the crystal-to-melt transition. Therefore, the heat of fusion ( $\Delta H$ ) indicated in Figure 6 consists of  $X_c$  plus  $X_s$ , i.e.  $\Delta H=(X_c+X_s)\Delta H_c^\circ$ , where  $\Delta H_c^\circ$  is the heat of fusion for the  $\alpha$ -crystal.  $\Delta H_s$  and  $\Delta H$  as a function of CR are plotted in Figure 7.  $\Delta H_s$  decreased with CR, suggesting that the amount of smectic

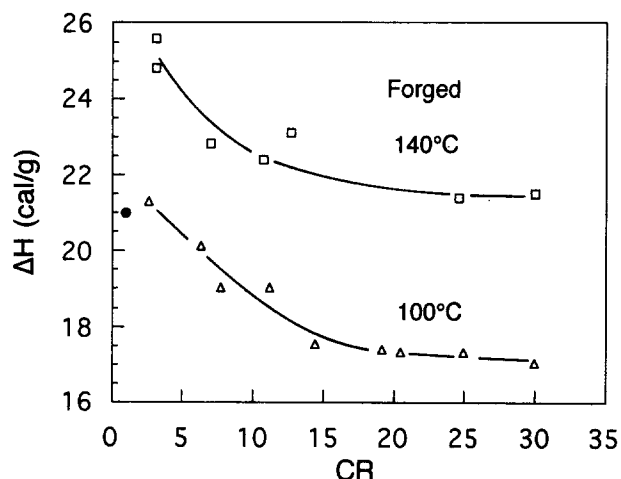


Figure 1  $\Delta H$  versus CR for samples prepared at 100 ( $\Delta$ ) and 140°C ( $\square$ ); original undeformed sample ( $\bullet$ )

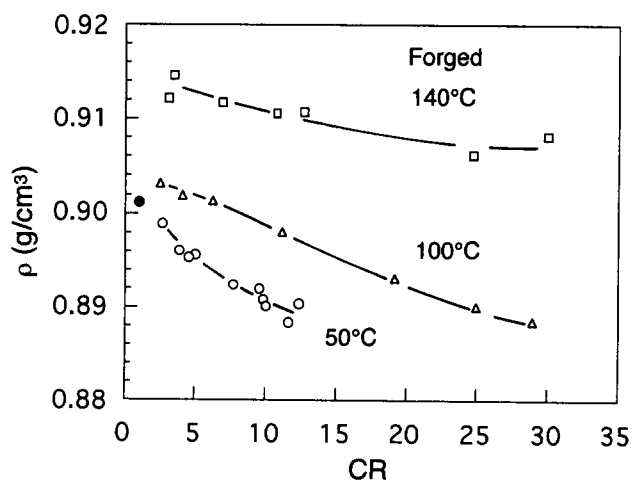
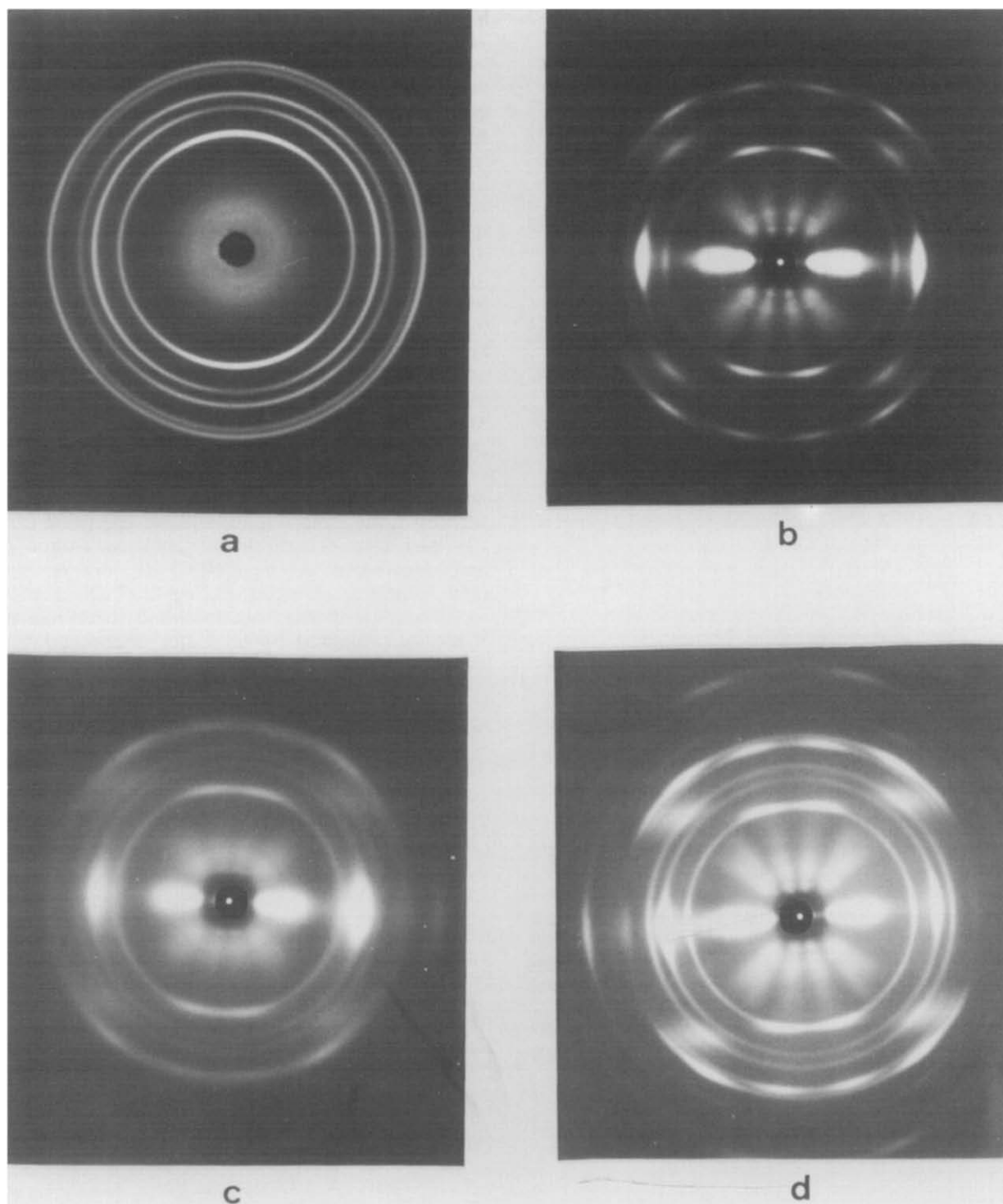


Figure 2 Density versus CR for samples prepared at 50 ( $\circ$ ), 100 ( $\Delta$ ) and 140°C ( $\square$ ); original undeformed sample ( $\bullet$ )



**Figure 3** WAXS patterns of samples prepared at different  $CR$  and  $T_d$ : (a)  $CR=3.9$  at  $140^\circ\text{C}$ , (b)  $CR=50$  at  $140^\circ\text{C}$ , (c)  $CR=12$  at  $50^\circ\text{C}$ , (d) sample c subsequently heat treated ( $140^\circ\text{C}$  for 30 min). The incident X-ray beam is parallel to the plane direction. The plane direction is vertical on the photographs

phase increased during the deformation. On the other hand,  $\Delta H$  is almost constant at  $CR < 4$ , suggesting only an  $\alpha$ -crystal-to-smectic transition in the initial stage of deformation. Subsequently, on draw, the smectic-to-amorphous transition may occur in addition to the  $\alpha$ -crystal-to-smectic transition. Although a qualitative estimation of the smectic-phase content has been reported<sup>7</sup>, the fraction of smectic phase could not be directly calculated from the exotherms, since the absolute heat for smectic-to- $\alpha$ -crystal transition is unknown. Since the peaks of  $\Delta H$  and  $\Delta H_s$  differ by  $\sim 80^\circ\text{C}$ ,  $X_c + X_s$  can

be estimated approximately from  $X_c + X_s = \Delta H / \Delta H_c^\circ$ , although the exotherm and endotherm probably overlap. As such, the above estimation combined with equation (2) gives  $X_s$ :

$$X_s = \frac{1/\rho - X_i(1/\rho_c - 1/\rho_a) - 1/\rho_a}{1/\rho_s - 1/\rho_c} \quad (3)$$

where  $X_i = X_c + X_s$ , and a value of  $\rho_s = 0.916 \text{ g cm}^{-3}$  is taken<sup>17</sup>. The  $\rho_a$  for  $T_d = 50^\circ\text{C}$  is still unknown. The  $\rho_a$  for  $T_d = 50^\circ\text{C}$  was estimated from the dotted line in Figure 8 (data are from Figure 6) since the values of  $\rho_a$

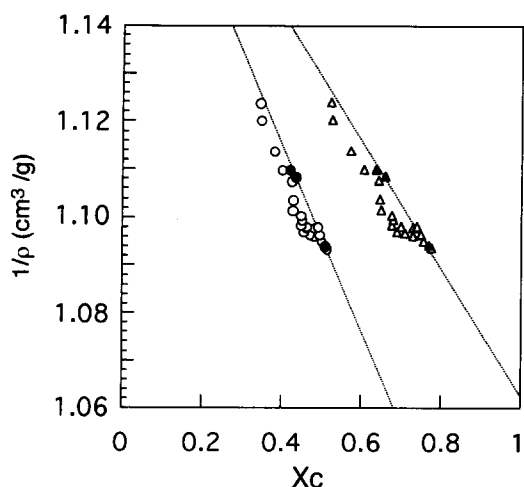


Figure 4  $1/\rho$  versus  $X_c$  calculated using  $\Delta H_c$  values of 50 (○) and 33 cal g<sup>-1</sup> (△). Filled symbols (●) for 50 and (▲) for 33 cal g<sup>-1</sup> are for undeformed samples with different crystallinity

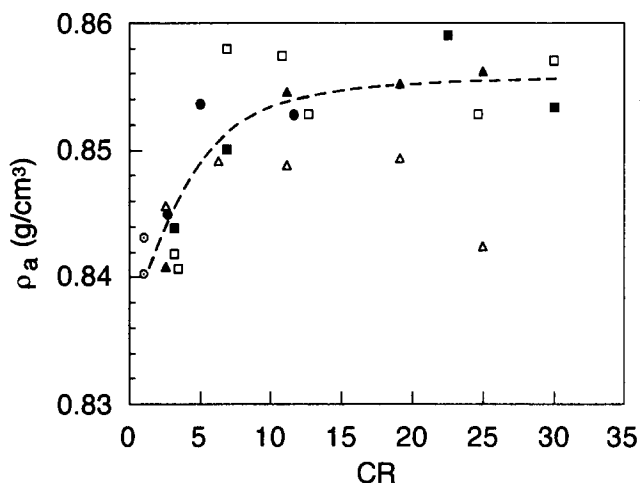


Figure 5 Amorphous density versus CR for samples prepared at 100 (△) and 140°C (□), and subsequently heat treated (140°C for 30 min) samples of  $T_d$  at 50 (●), 100 (▲) and 140°C (■)

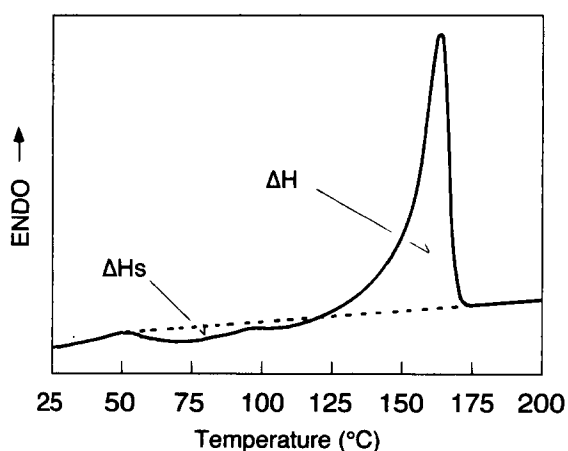


Figure 6 D.s.c. thermogram for the sample prepared at 50°C for CR=10

estimated in Figure 6 were a function of CR (independent of  $T_d$ ). The calculated weight fractions  $X_s$ ,  $X_c$  and  $X_a$  as a function of draw are shown in Figure 9a. For a CR up to 10, a large fraction of the  $\alpha$ -crystal transforms to the smectic phase. This is confirmed by the broad and weak WAXS pattern of the sample drawn at 50°C (see

Figure 3c). The average heat of transition for smectic to  $\alpha$ -crystal estimated from Figures 7 and 9a was  $\sim 5.5$  cal g<sup>-1</sup>. This value is quite low compared with that for an  $\alpha$ -crystal-to-melt transition because the smectic phase is a disordered form of the  $\alpha$ -crystal, and smectic and  $\alpha$ -crystal involve a one-three helix<sup>18</sup>. Thus, the smectic phase can easily revert back to the  $\alpha$ -crystal on heating.

Figure 10 is a schematic of the phase changes on draw for  $T_d < T_s$ . At  $T_d$  (50°C)  $< T_s$ , it is thought that the crystal deformation proceeds through the generation of an intermediate smectic phase (Process I). Figure 9a shows that a large fraction of  $\alpha$ -crystal is transformed to smectic by a CR of  $\sim 10$ . In this process, the molecular chains are pulled out from the lamellae (lamellae unravelling process). For  $T_d = 100^\circ\text{C}$ , the smectic phase cannot be observed. However, Process I would also proceed since the smectic phase is produced during the deformation<sup>7</sup>. After compression, the smectic phase reverts back to the  $\alpha$ -crystal (Process I') because the smectic phase is unstable at  $> 70^\circ\text{C}$  and atmospheric pressure<sup>7,19</sup>. In addition to Process I, the smectic-to-amorphous transition (Process II) may also occur, but the process is not major (see Figure 9a). At  $T_d$  (140°C)  $> T_s$ , decrystallization and annealing proceed during the deformation. A small amount of  $\alpha$ -crystal was totally decrystallized by CR  $< \sim 10$  followed by no major decrystallization on further draw (see Figure 9b). At this temperature, however, the metastable smectic phase is not formed<sup>7</sup>, so that the

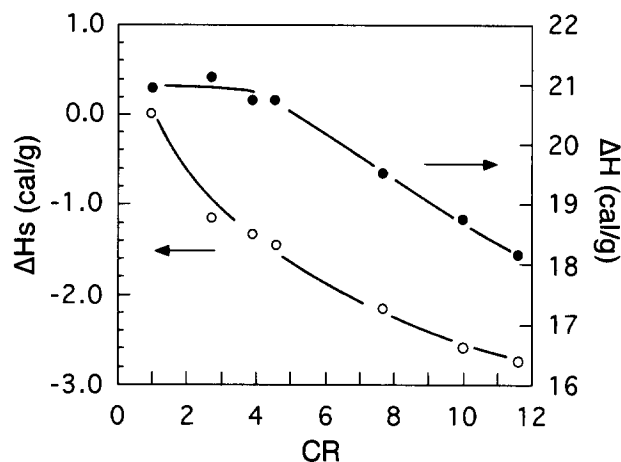


Figure 7  $\Delta H_s$  and  $\Delta H$  versus CR for samples prepared at 50°C

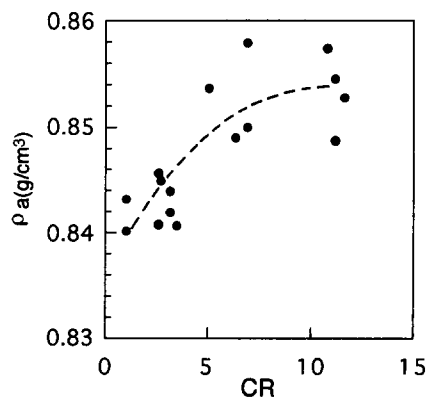


Figure 8  $\rho_a$  versus CR: dotted line is expressed by  $\rho_a = 0.836 + 3.40 \times 10^{-3} \times CR - 1.65 \times 10^{-4} CR^2$

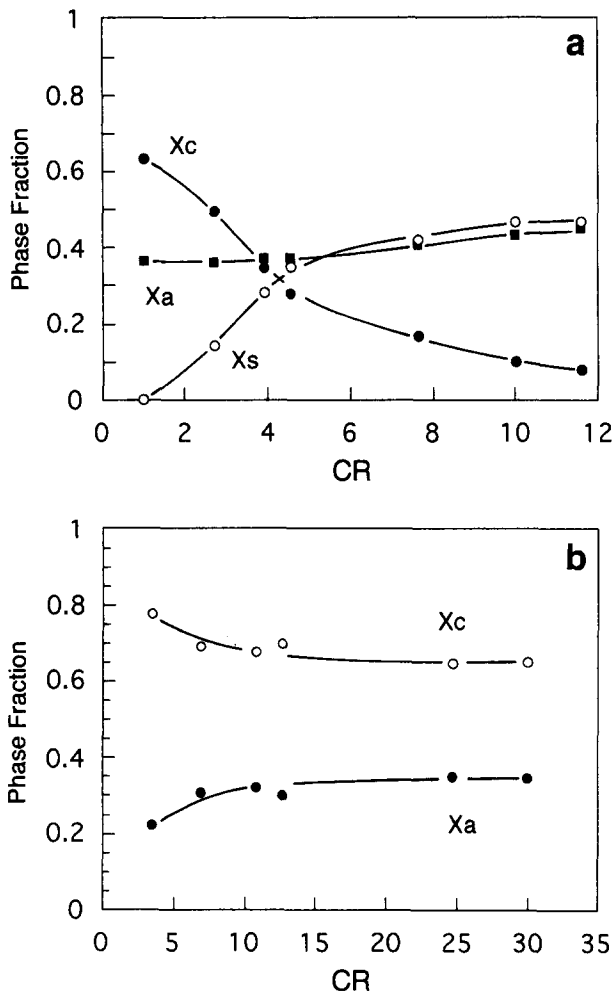


Figure 9 (a)  $X_c$  (●),  $X_s$  (○) and  $X_a$  (■) as a function of CR for samples prepared at 50°C; (b)  $X_c$  (○) and  $X_a$  (●) as a function of CR for samples prepared at 140°C

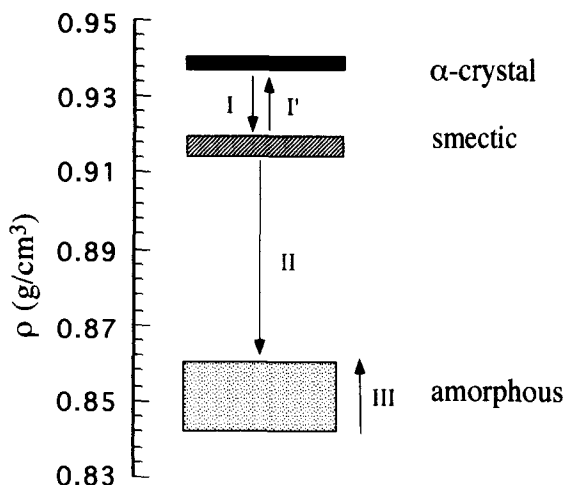


Figure 10 Schematic of phase changes on compression draw

pulled-out chains fall back into their  $\alpha$ -crystal form during the deformation, prohibiting the lamellae unravelling process. We have reported<sup>8</sup> that the draw efficiency parallel to the uniplanar direction for  $T_d < T_s$  was higher than that for  $T_d > T_s$ . It can thus be concluded that Process I apparently facilitates the efficient draw of the  $\alpha$ -crystal phase.

The original undeformed iPP sample consists of about half amorphous chains. During the sample deformation, the amorphous chains are extended by the compressive force. Saraf and Porter<sup>7</sup> pointed out that the amorphous region might form a rubbery network with entanglement points as temporary crosslink junctions<sup>20</sup>. Furthermore, the network might behave like an ideal rubber for planar deformation up to  $\sim 4^{7,21}$ . As shown in Figure 5, the amorphous density increased rapidly at low CR ( $< \sim 5$ ). This indicates that the rubber-like deformation of the amorphous phase is accompanied by an increase in the density caused by the compressive force. Process III is independent of  $T_d$ . Therefore, there seems to be no relation between the increase in amorphous density and the formation of the smectic phase.

The uniplanar deformed iPP samples showed some interesting properties and morphology. For example,  $T_g$  increased with draw, the smectic phase reduced the tensile modulus, the transparency of the sample was improved with the existence of the smectic phase, and the deformed sample had a layer structure. The effects of structural change on the physical properties of iPP will be reported in a subsequent paper.

## CONCLUSION

The uniaxially compressed iPP consisted of two or three phases ( $\alpha$ -crystal and amorphous or  $\alpha$ -crystal, amorphous and smectic), depending on the draw temperature ( $T_d$ ). The percentage of each phase and amorphous density increase have been evaluated by thermal analysis and density measurements. At  $T_d < T_s$ , a large fraction of the  $\alpha$ -crystal transforms to the smectic phase by a CR of  $\sim 10$ , without any major change in the amorphous fraction. This process facilitates lamellae unravelling, leading to a high molecular draw efficiency. At  $T_d > T_s$ , no measurable smectic fraction is observed. The density of the amorphous phase increases with increasing CR up to  $\sim 10$ , independent of  $T_d$ .

## ACKNOWLEDGEMENT

The authors thank the National Science Foundation for support through CUMIRP at the University of Massachusetts.

## REFERENCES

- Zachariades, A. E. and Porter, R. S. (Eds) 'Strength and Stiffness of Polymers', Vol. 4, Plastic Engineering Series, Marcel Dekker, New York, 1983
- Inoue, N. and Ichihara, M. (Eds) 'Hydrostatic Extrusion; Theory and Applications', Elsevier, London, 1985
- Kanamoto, T., Tsuruta, A., Tanaka, K. and Takeda, M. *Polym. J.* 1984, **16**, 75
- Peguy, A. and Manley, R. St. J. *Polym. Commun.* 1984, **25**, 39
- Matsuo, M., Sawatari, C. and Nakano, N. *Polym. J.* 1986, **18**, 75
- Saraf, R. F. and Porter, R. S. *J. Rheol.* 1987, **31**, 59
- Saraf, R. F. and Porter, R. S. *Polym. Eng. Sci.* 1988, **28**, 842
- Osawa, S. and Porter, R. S. *Polymer* 1994, **35**, 540
- Saraf, R. F. and Porter, R. S. *Mol. Cryst. Liq. Cryst. Lett.* 1985, **2(3-4)**, 85
- Samuels, R. J. 'Structured Polymer Properties', Wiley, New York, 1974
- Taraiya, A. K., Unwin, A. P. and Ward, I. M. *J. Polym. Sci. Polym. Phys. Ed.* 1988, **26**, 817
- Matsuo, M., Sawatari, C. and Nakano, T. *Polym. J.* 1986, **18**, 759

*Uniplanar deformation of iPP. 2: S. Osawa and R. S. Porter*

- |    |  |    |  |
|----|--|----|--|
| 13 | Roy, S. K., Kyu, T. and Manley, R. St. J. <i>Macromolecules</i> 1988, <b>21</b> , 499            | 17 | Brandrup, J. and Immergut, E. H. 'Polymer Handbook', 3rd Edn, Wiley, New York, 1989                      |
| 14 | Fatou, J. G. <i>Eur. Polym. J.</i> 1971, <b>7</b> , 1057   | 18 | Miller, R. L. <i>Polymer</i> 1960, <b>1</b> , 135  |
| 15 | Wunderlich, B. 'Macromolecular Physics', Vol. 3, Crystal Melting, Academic Press, New York, 1980 | 19 | Zannetti, R., Celotti, G., Fichera, A. and Francesconi, R. <i>Makromol. Chem.</i> 1969, <b>128</b> , 137 |
| 16 | Osawa, S., Porter, R. S. and Ito, M. <i>Am. Chem. Soc., PMSE Prepr.</i> 1992, <b>67</b> , 278    | 20 | Graessley, W. W. <i>Adv. Polym. Sci.</i> 1974, <b>16</b> , 1   |
|    |  | 21 | Treloar, L. R. G. <i>Trans. Faraday Soc.</i> 1946, <b>42</b> , 83  |